International Immunopharmacology 136 (2024) 112273

Contents lists available at ScienceDirect

International Immunopharmacology

journal homepage: www.elsevier.com/locate/intimp

Precision immunotherapy for cholangiocarcinoma: Pioneering the use of human-derived anti-cMET single chain variable fragment in anti-cMET chimeric antigen receptor (CAR) NK cells

Chutipa Chiawpanit [a,b,c], Methi Wathikthinnakorn [d], Nunghathai Sawasdee [e], Nattaporn Phanthaphol [f], Jatuporn Sujjitjoon [e], Mutita Junking [e], Montarop Yamabhai [g], Jutatip Panaampon [h], Pa-thai Yenchitsomanus [e], Aussara Panya [a,b,*]

[a] Cell Engineering for Cancer Therapy Research Group, Chiang Mai University, Chiang Mai, Thailand
[b] Department of Biology, Faculty of Science, Chiang Mai University, Chiang Mai, Thailand
[c] Office of Research Administration, Chiang Mai University, Chiang Mai, Thailand
[d] Department of Veterinary and Animal Sciences, Faculty of Health and Medical Sciences, University of Copenhagen, Copenhagen, Denmark
[e] Siriraj Center of Research Excellence for Cancer Immunotherapy (SiCORE-CIT), Research Department, Faculty of Medicine, Siriraj Hospital, Mahidol University, Bangkok, Thailand
[f] College of Medical, Veterinary and Life Sciences, University of Glasgow, Glasgow, Scotland, United Kingdom
[g] Molecular Biotechnology Laboratory, School of Biotechnology, Institute of Agriculture Technology, Suranaree University of Technology, Nakhon Ratchasima, Thailand
[h] Department of Medical Oncology, Dana-Farber Cancer Institute, Harvard Medical School, Boston, MA, USA

ARTICLE INFO

Keywords:
Cholangiocarcinoma
cMET
Natural killer cells
Chimeric antigen receptor
Single chain variable fragment

ABSTRACT

Cholangiocarcinoma (CCA) presents a significant clinical challenge which is often identified in advanced stages, therby restricting the effectiveness of surgical interventions for most patients. The high incidence of cancer recurrence and resistance to chemotherapy further contribute to a bleak prognosis and low survival rates. To address this pressing need for effective therapeutic strategies, our study focuses on the development of an innovative cellular immunotherapy, specifically utilizing chimeric antigen receptor (CAR)-engineered natural killer (NK) cells designed to target the cMET receptor tyrosine kinase. In this investigation, we initiated the screening of a phage library displaying human single-chain variable fragment (ScFv) to identify novel ScFv molecules with specificity for cMET. Remarkably, ScFv11, ScFv72, and ScFv114 demonstrated exceptional binding affinity, confirmed by molecular docking analysis. These selected ScFvs, in addition to the well-established anti-cMET ScFvA, were integrated into a CAR cassette harboring CD28 transmembrane region-41BB-CD3ζ domains. The resulting anti-cMET CAR constructs were transduced into NK-92 cells, generating potent anti-cMET CAR-NK-92 cells. To assess the specificity and efficacy of these engineered cells, we employed KKU213A cells with high cMET expression and KKU055 cells with low cMET levels. Notably, co-culture of anti-cMET CAR-NK-92 cells with KKU213A cells resulted in significantly increased cell death, whereas no such effect was observed with KKU055 cells. In summary, our study identified cMET as a promising therapeutic target for CCA. The NK-92 cells, armed with the anti-cMET CAR molecule, have shown strong ability to kill cancer cells specifically, indicating their potential as a promising treatment for CCA in the future.

1. Introduction

Cholangiocarcinoma (CCA) is a highly aggressive biliary adenocarcinoma [1], with over 70 % of patients on the globe diagnosed with the extrahepatic subtype [2]. Notably, there is a growing incidence of intrahepatic CCA, particularly in East Asian countries [1] and conventional therapy for this condition involving surgical resection is associated with higher recurrence rates (60–90 %) and poor 5-year survival rates [2]. Additionally, surgical resection is not feasible for patients in advanced stage (70–80 %), leaving them with limited treatment options. While a combination of gemcitabine and cisplatin chemotherapy has emerged as a first-line treatment option, it only

* Corresponding author at: Department of Biology, Faculty of Science, Chiang Mai University, 293, Hauy Kaew Road, Muang District, Chiang Mai 50200, Thailand.
E-mail address: aussara.pan@cmu.ac.th (A. Panya).

https://doi.org/10.1016/j.intimp.2024.112273
Received 31 December 2023; Received in revised form 13 May 2024; Accepted 13 May 2024
Available online 28 May 2024

extends survival by a one-year period [3,4]. Moreover, the disruption of immunosurveillance, a crucial immune mechanism responsible for eliminating cancer cells through natural killer (NK) and T cells, is a feature in CCA. This disruption is primarily attributed to immune escape mechanisms and alterations in the tumor microenvironment [5]. Consequently, immunotherapy, which enhances the killing efficacy and specificity of the immune cells against cancer cells, has emerged as a viable solution to counter the immune escape mechanism and represents a promising alternative therapy for CCA [6].

Immunotherapy approaches, encompassing immune checkpoint modulators targeting CTLA-4 and PD-1, as well as adoptive cell therapy utilizing natural killer (NK) and T cells, exhibit potential in augmenting the anti-tumor efficacy of cytotoxic immune cells against cancer [5]. Notably, the adoptive cell transfer of genetically engineered cytotoxic immune cells equipped with chimeric antigen receptor (CAR) holds greater promise for cancer treatment [7,8]. CAR-engineered cytotoxic T (CAR-T) cells, specifically targeting CD19, have received approval for hematological malignancies and include treatments with the brand names Kymriah [9,10], Yescarta [11], Breyanzi [12], and Tecartus [13]. Additionally, Abecma has been approved for treating multiple myeloma by targeting BMCA [14]. However, their application in treating tumors has been constrained by adverse side effects such as cytokine release syndrome (CRS), graft versus host disease (GVHD), and challenges posed by the formidable tumor microenvironment hindering CAR efficacy against solid tumors [15,16]. In contrast, NK cells, an integral member of the innate immune system, present a promising alternative for cancer treatment. The infusion of NK-92 cells in cancer patients has demonstrated encouraging outcomes with fewer side effects and a lower risk of graft-versus-host disease (GVHD) [8] and the avoidance of cytokine release syndrome (CRS) and neurotoxicity [17]. Notably, the cytotoxicity of NK cells is initiated through an MHC-independent mechanism involving recognition and activation by various mechanisms, such as antibody-dependent cellular cytotoxicity (ADCC) and the association/disassociation of activating and inhibitory molecules. These characteristics position NK cells as a potential model for the development of off-the-shelf CAR-based adoptive cell immunotherapy for CCA [17].

The proto-oncogene mesenchymal-epithelial transition (MET/cMET/c-Met/HGFR) protein has been implicated in various cancers, including pancreatic [18], breast [19], cervical [20], gastrointestinal [21], and CCA [22–24]. The cMET expression in CCA tissue was variable between different studies depending on several factors including population, CCA type, treatment history, and stage of disease. Wei et al. studied cMET expression in twenty-three corresponding tumor- and non-tumor tissues that were collected from patients with intrahepatic (iCCA) and perihilar CC (pCCA) [22]. Notebly, 91.3 % of tumor tissue samples (21/23) had c-MET overexpression that was not detected in the corresponding non-tumor tissues [22]. A cohort study that recruited 291 resected specimens in China demonstrated a concordant result in which high cMET expression was found in 53.1 % (135 of 254) of samples [23]. Importantly, high cMET expression correlated with disease prognosis where patients with high expression had significant shorter overall survival (OS) rates and disease-free survival (DFS) rates than those with low cMET expression (OS 15.00 months versus mean 27.47 months; DSF 12.00 months versus 30.80 months based on univariate analysis) [23]. Furthermore, the immunohistochemical analysis of cMET on CCA tissues from 247 cases enrolled in the National Cancer Center Hospital, Tokyo showed positive staining for cMET in 143 of the 247 cases (57.9 %) including 50 of the 111 iCCA cases and (45.0 %) and 93 of the 136 extrahepatic (eCCA) cases. Interestingly, the cMET expression level was also negatively correlated with the five-year survival rate. The iCCA patients with high and low cMET expression had five-year survival of 15.4 % and 41.1 %, respectively, where the survival was higher in eCCA patients with 40.9 % and 45.8 %, respectively [24,25]. Based on these previous reports, targeting cMET has therefore emerged as a promising approach for cancer therapy [26]. Recently, the development of a cell-based immunotherapy involving chimeric antigen receptor (CAR) natural killer (NK) cells targeting cMET provided promising outcomes in lung cancer [27] and liver cancer models [28]. The cMET-CAR-NK cells, designated as CCN4, incorporating DAP10 co-stimulation, exhibited anti-tumor activity against cMET-positive H1299 cells and has effectively inhibited tumor growth in xenograft models [27]. Furthermore, primary NK cells expressing cMET-CAR demonstrated a strong cytotoxicity against HepG2 cells with high cMET expression over the H1299 cells, highlighting the feasibility of utilizing cMET-CAR-NK to target cancer cells, particularly those with elevated cMET levels [28]. Notably, NK killing activity in target cells also depended on balancing the activating and inhibitory signals. The magnitude of CAR-NK efficiency not only depends on the cMET expression level but might be influenced by the genetic background and inherent characteristics of the target cells, leading to variable responses, particularly in cancers with highly heterogeneity or across different cancer types.

While the overexpression of cMET in CCA is well documented, there has been no work demonstrating the efficiency of CAR-NK targeting cMET in CCA. Therefore, acknowledging the potential significance of cMET as a therapeutic target, we aimed to investigate the efficiency of anti-cMET CAR-NK-92 cells against CCA, which often exhibits high heterogeneity and therapy resistance. This technology holds promise for improving outcomes in CCA treatment. In this study, a novel humanized single-chain variable fragments (ScFvs) that specifically targets cMET was identified. Such ScFvs offer alternative options for multi-epitope targeting to prevent escape via mutation and enable exploration of their functionality in the development of anti-cMET CAR-NK-92 cell therapy for treating CCA. In this investigation, the identified ScFvs were genetically integrated into a CAR construct, encompassing a CD28 transmembrane domain, a 41BB co-stimulatory domain, and a CD3ζ signaling domain. Our study is the first to demonstrate the potent killing efficacy of anti-cMET CAR-NK-92 cells against CCA cell lines, exhibiting high specificity for cancer cells expressing cMET.

2. Materials and methods

2.1. Cell culture

The CCA cell lines, KKU055, KKU100, KKU213A, KKK-D068, KKK-D131, and KKK-D138 derived from CCA patients in Northeastern Thailand, in addition to, RBE, SSP25, and YSCCC were procured from Japanese Collection of Research Bioresources Cell Bank (JCRB Cell Bank). These cells were cultured at 37 °C with 5 % CO_2 in DMEM-F12 (Thermo Fisher Scientific, Waltham, MA, USA) supplemented with 10 % fetal bovine serum (FBS) (Thermo Fisher Scientific, Waltham, MA, USA). Similarly, HEK293T and Lenti-X^{TM} 293 T cells (Takara Bio, CA, USA) followed the same culture conditions as CCA cell lines. Additionally, NK-92 cells (ATCC, Manassas, VA, USA) were cultured in alpha minimum essential medium without ribonucleosides and deoxyribonucleosides (Thermo Fisher Scientific, Waltham, MA, USA) supplemented with 2 mM L-glutamine, 1.5 g/L sodium bicarbonate, 0.02 mM inositol, 0.1 mM 2-mercaptoethanol, 0.02 mM folic acid, 100–200 U/ml recombinant IL-2 (R & D system, Minneapolis, MN, USA), 12.5 % horse serum, and 12.5 % FBS (Thermo Fisher Scientific, Waltham, MA, USA).

2.2. Immunoblot assay

An immunoblot analysis was employed to assess cMET protein expression levels in CCA cell lines (KKU055, KKU100, and KKU213A). The cell lines were lysed with RIPA buffer, and the optimal cell number for lysate preparation was 1×10^6 cells per cell line. Following incubation on ice for 30 min, centrifugation at 12,000 rpm for 10 min removed cell debris from the supernatant. Cell lysates were loaded onto 12 % sodium dodecyl sulfate–polyacrylamide gel electrophoresis (SDS-PAGE), transferred to a nitrocellulose membrane, and blocked with 5 % skimmed milk for 1 h. The membrane was then incubated with rabbit anti-cMET primary antibody (1:1000) (ABclonal, Woburn, MA, USA) at

4 °C overnight. After three washes with 0.1 % TBST, the membrane was incubated with a goat anti-rabbit secondary antibody (1:1000) (ab51067, Abcam) for 1 h. The membrane was washed three times with 0.1 % TBST. The expression signal was detected using West Pico PLUS Chemiluminescent Substrate (Thermo Fisher Scientific, Waltham, MA, USA), and cMET protein abundance was quantified with the ImageQuant LAS 500 Chemiluminescent Imaging System (GE, Boston, MA, USA).

In a separate analysis, anti-cMET ScFvs in bacterial cultured supernatants were detected by immunoblot assay. Whole cell suspension and supernatant from each bacterial colony were loaded into 12 % SDS-PAGE and transferred to the nitrocellulose membrane. Anti-cMET ScFv expression was detected using a 1:1000 dilution of 6x-His Tag primary antibody (Invitrogen, CA, USA).

Furthermore, the expression of anti-cMET CAR constructs was evaluated using immunoblot assay. The expressed CAR was visualized using a mouse anti-MYC tag (1:1000) (Invitrogen, CA, USA) and compared with the endogenous expression of GAPDH (rabbit anti-GAPDH; 1:100) (ABclonal, Woburn, MA, USA).

2.3. Immunofluorescence assay

The expression and localization of cMET were demonstrated by an immunofluorescence assay (IFA). Initially, CCA cells (6×10^5 cells/well) were seeded onto 6-well culture plate with a glass coverslip and incubated at 37 °C with 5 % CO_2 overnight until reaching 70–90 % confluence. The cultured medium was then removed, and cells were gently washed once with 1 ml of PBS. Subsequently, cells were fixed with 0.5 ml of 4 % paraformaldehyde in PBS at room temperature for 15 min, followed by three washes with PBS. After fixation, the cells were permeabilized with 0.5 ml of 0.1 % Triton X-100, incubated at room temperature for 15 min, and washed twice. Permeabilized cells on coverslips were transferred to 24-well plate, and a blocking step was performed by adding 0.2 ml of 5 % bovine serum albumin (BSA), incubating for 15 min at room temperature. Rabbit anti-cMET (ab51067, Abcam) in a 1:500 dilution was added after removing the blocking buffer, and the incubation step was carried out at 37 °C for an hour, followed by three washing steps. Alexa Fluor 555 conjugated Donkey anti-rabbit (A32794) in a 1:1000 dilution containing Hoechst 33,342 (1:1000) was added and incubated in the dark at 37 °C for 30 min. After three additional washing steps, 10 μl of mounting media was added to microscope slide to mount the coverslip. The edge of the coverslip was sealed with clear nail polish and allowed to dry. IFA results were observed and captured under a confocal microscope.

The assessment of anti-cMET CAR construct expression in HEK293T cells was conducted using an immunofluorescence assay (IFA). Following transfection, HEK293T cells were fixed with 3.6 % formaldehyde for 15 min, followed by a washing step with 0.1 % PBST. A blocking step, employing 2 % BSA for one hour at room temperature was then undertaken. Subsequent washes with 0.1 % PBST were performed, and then a mouse anti-MYC tag antibody (1:500) (Invitrogen, CA, USA) was added, and incubated at 37 °C for 2 h. Post-incubation, the primary antibody was removed, and the cells were washed with 0.1 % PBST. Goat anti-mouse Alexa Fluor 488 secondary antibody (Invitrogen, CA, USA) at a 1:500 dilution, along with Hoechst (1:1000), was applied to the well, followed by a 45-minute incubation in a dark place at room temperature. Results were observed using a fluorescent inverted microscope.

2.4. Flow cytometry

Flow cytometry was conducted to validate the cMET protein expression on the surface of CCA cells. The CCA cell lines were harvested and washed with PBS containing 2 % fetal bovine serum (FBS). Subsequently, the collected cells were incubated with anti-human cMET antibody conjugated to APC fluorescence (1:100) (ABclonal, Woburn, MA, USA) and placed on ice for 30 min in a dark environment. After staining, the cells were washed twice with PBS containing 2 % FBS and analyzed using the BD Accuri™ C6 Flow Cytometer (BD Biosciences, San Joes, CA, USA).

Additionally, the surface expression of the anti-cMET CAR on HEK293T and NK-92 cells was confirmed through flow cytometry using mouse anti-MYC tag conjugated FITC (1:100). Analysis was performed using the BD Accuri™ C6 Flow Cytometer (BD Biosciences, San Joes, CA, USA).

2.5. Screening of novel human Anti-cMET ScFvs

Bacterial cells infected with the YAMO1 human ScFv library-containing phage [29] were subjected to colony polymerase chain reaction (PCR) using LMB3-F and pHEN-R primers (Supplementary Table 1) to amplify the ScFv domain. The resulting PCR products were digested with the BstNI restriction enzyme to examine ScFv variation, with the digestion reaction carried out at 60 °C for 3 h. The patterns of digested PCR products were observed using 3 % agarose gel electrophoresis utilising U:GENIUS^3 (Syngene, Cambridge, UK).

In screening ScFv expression targeting cMET, bacterial colonies infected through phage display and bio-panning were cultured in LB low salt medium supplemented with 100 μg/ml ampicillin at 37 °C with 250 rpm overnight. The bacterial suspension was then inoculated into freshly prepared LB low salt medium supplemented with 100 μg/ml ampicillin and incubated at 37 °C with 250 rpm until it reached the log phase of growth. Subsequently, 1 mM IPTG was added to the bacterial suspension, and further incubation undertaken at 30 °C with 250 rpm overnight to enable bacterial expression and secretion of the ScFv targeting cMET. Finally, the bacterial suspension was collected by centrifugation at 8,000 rpm at 4 °C. The supernatant containing the ScFv protein was utilized for protein expression detection via immunoblot analysis and stored at −20 °C until use.

2.6. Enzyme-linked immunosorbent assay (ELISA)

Enzyme-linked immunosorbent assay (ELISA) was employed to assess the recognition properties of candidate ScFvs against cMET recombinant proteins. The cMET recombinant protein was coated onto a 96-well plate with coating buffer and incubated at 4 °C overnight. After this incubation period, the wells were washed with PBS containing 0.1 % Tween 20 (0.1 % PBST). The plate was then blocked with 2 % BSA for 1 h at 37 °C, followed by three washes with washing buffer (0.1 % TBST). Supernatant containing ScFv proteins were added to each well and incubated at 37 °C for 3 h. After three washes, the plate was treated with tetramethyl benzidine (TMB) substrate (Invitrogen, CA, USA), and the signal was detected at OD 650 nm using the NS-100 NanoScan Microplate Reader (Hercuvan Lab System, Cambridge, UK).

To assess the efficiency of individual purified ScFvs in binding to cMET expressed on CCA cell lines, specifically comparing between KKU055 (lowest cMET expression) and KKU213A (highest cMET expression), an ELISA assay was conducted. Briefly, KKU055 and KKU213A (7×10^3 cells/well) were plated on a 96-well plate for 24 h. Before the ELISA, the cells were washed with PBS and fixed with 3.6 % formaldehyde in PBS for 15 min at room temperature. After a PBS wash, the cells were blocked with 1 % BSA in PBS for 1 h at 37 °C. Following another PBS wash, undiluted purified ScFvs (ScFv11 and ScFv72) were added to the wells and incubate at 37 °C for 2 h. The subsequent washing step was performed three times using 0.05 % PBST. Mouse anti-MYC antibody (1:1,000 in 2 % BSA) (Invitrogen, CA, USA) was added and incubated at 37 °C for 2 h, followed by three washes. Rabbit anti-mouse (1:1,000 in 2 % BSA) (ABclonal, Woburn, MA, USA) was then added, and after a 30-minute incubation at 37 °C, three additional washes were performed. Tetramethyl benzidine (TMB) (Invitrogen, CA, USA) was added (100 μl/well) and incubated in the dark at room temperature until the solution turned blue. Recognition was evaluated at an absorbance of

650 nm using the NS-100 NanoScan Microplate Reader (Hercuvan Lab System, Cambridge, UK).

2.7. Protein purification and measurement

Positive infected bacterial clones capable of expressing ScFv targeting cMET were purified using TALON® metal affinity resin (Takara Bio, CA, USA). The supernatant containing ScFv targeting cMET was combined with a buffer containing TALON beads and allowed to interact for 3 h. The bound ScFvs were then eluted using an elution buffer with 50 mM imidazole. To assess the concentration of purified anti-cMET ScFv, a Bradford assay (Bio-Rad, Hercules, CA, USA) was performed.

2.8. Molecular docking

Molecular interactions between ScFvs and the cMET protein were assessed through molecular docking analysis. The putative 3D structures of both ScFvs and the cMET protein were obtained via homology remodeling using the SWISS model web server [30]. Subsequently, they were employed in simulating protein–protein interactions using the ZDOCK [31] and HADDOCK [32] programs. The calculated binding affinity of the ScFvs was then evaluated and compared with the biological activity of cMET.

2.9. Production of anti-cMET CAR-NK-92 cells

Candidate scFvs targeting cMET were genetically engineered to fuse with a CAR cassette, with the VH-linker-VL fragment incorporated in-frame with the CD28-41BB-CD3ζ portion of the pcDH vector backbone, resulting in the production of anti-cMET CAR constructs (Fig. 5A–B). The expression of CAR constructs was confirmed through transfection into HEK293T cell lines using lipofectamine 2000 (Invitrogen, Life Technologies, Carlsbad, CA, USA).

Positively expressed CAR constructs (A-CAR2, 11-CAR2, and 72-CAR2) were then transduced into NK-92 cells using lentivirus to generate CAR-NK-92 cells targeting cMET. Briefly, Lenti-X^{TM} 293 T cells (5×10^6 cells) were plated on a 10 cm culture dish for 24 h. The anti-cMET CAR plasmids (transfer plasmid) were co-transfected with lentiviral packaging plasmid, pMD2.G and psPAX2, in a ratio of transfer: pMD2.G:psPAX2 equal to 5:1:3, respectively, using the $CaCl_2$ method. Supernatants containing lentiviruses were collected after 48 h after the co-transfection step and filtered through a 0.45 μm PES membrane filter. The lentiviruses were concentrated by ultracentrifugation at 20,000×g for 90 min at 4 °C. After the centrifugation, the supernatant was discarded, and the pellet of concentrated lentiviruses was resuspended in NK-92 culture media. The transduction procedure was subsequently carried out by culturing NK-92 cells (5×10^5 cells/CAR construct) in a 12-well plate with resuspended lentivirus containing protamine sulfate (10 μ/ml) and spinoculating the plate at 1,200×g, 32 °C for 90 min. Finally, the culture plate was incubated at 37 °C under a humidified 5 % CO_2 atmosphere for 24 h. A second round of transduction was also performed. After the second transduction, the expression of anti-cMET CAR on NK-92 cells was evaluated by detecting the c-MYC tag in a 1:100 dilution on the ScFv domain using a BD Accuri^{TM} C6 Flow Cytometer (BD Biosciences, San Joes, CA, USA). The timeline of lentivirus production and the transduction procedure is indicated in Fig. 6A.

2.10. Killing assay

Target cells (KKU055 and KKU213A) were seeded in a 96-well plate at a density of 10^4 cells/well and allowed to adhere for 24 h before coculturing with anti-cMET CAR-NK-92 cells. On the subsequent day, anti-cMET CAR-NK-92 cells were incubated with the target cells at various effector-to-target (E:T) ratios of 0.5:1, 1:1, and 2:1. The cytotoxic activity of anti-cMET CAR-NK-92 cells against cMET-expressing target cells was assessed using crystal violet staining. Viable target cells stained with crystal violet were solubilized with absolute methanol, and the absorbance was measured at 570 nm using the NS-100 NanoScan Microplate Reader (Hercuvan Lab System, Cambridge, UK). The percentage of cell death was calculated using the following equation:

$$\text{Cell death (\%)} = 100 - [(\text{OD570 of target cell cocultured with the CAR} - \text{NK} - 92 \text{ cells} / \text{OD570 of target cell alone}) \times 100]$$

2.11. Statistical analysis

Each experiment in this study was conducted in triplicate (N = 3) and is presented as the mean ± standard error of the mean (SEM). Statistic comparisons were generally conducted using One-way ANOVA from GraphPad Prism software, version 7.0a (GraphPad Software, Inc., San Diego, CA, USA).

3. Results

3.1. Variation in cMET expression levels among CCA cell lines

The CCA cases in Thailand have been extensively linked to the infections by liver flukes, particularly *Opisthochis vivierini,* which has contributed to its localized prevalence in this region. Thus, despite previous reports of cMET overexpression, we conducted the investigation into cMET expression in CCA cell lines derived from Thai patients. An immunoblotting assay was conducted to detect total cMET expression and to compare expression levels among three different cell lines: KKU055, KKU100, and KKU213A. The results revealed the presence of the cMET protein with a size of 145 kDa in all three cell lines. Notably, KKU213A exhibited the highest expression, followed by KKU100 and KKU055, respectively (Fig. 1A). To complement the immunoblotting data, an IFA was performed to visualize protein expression and elucidate its subcellular localization. The IFA results provided compelling evidence that KKU213A had the most significant abundance of cMET protein, predominantly localized to the cell membrane (Fig. 1B). In contrast, KKU100 and KKU055 exhibited moderate and low levels of expression, respectively, with cMET predominantly found in the cytoplasm (Fig. 1B). Furthermore, our findings from flow cytometry analysis were consistent with these results (Fig. 1C–D, Supplementary Figure1, and Supplementary Table 2). Specifically, the expression levels of cMET on the cell surface were quantified as follows: 91.77±4.33 % for KKU213A, 21.07±2.86 % for KKU100, and 0.88±0.62 % for KKU055.

3.2. Novel humanized anti-cMET ScFvs specifically bind to cMET proteins on CCA cells

Bio-panning of the humanized ScFv phage display library (Fig. 2A) was conducted to identify novel anti-cMET ScFvs specifically targeting the cMET recombinant protein. The selected phagemid clones were characterized using PCR-restriction fragment length polymorphism (RFLP), and the ScFv PCR products demonstrated an approximate length of 850 bp (Fig. 2B). RFLP analysis revealed that 14 clones exhibited distinct patterns after digestion with restriction enzymes (Fig. 2C). These 14 phagemid clones were confirmed for their expression of ScFv and tested for their binding to the cMET recombinant protein as

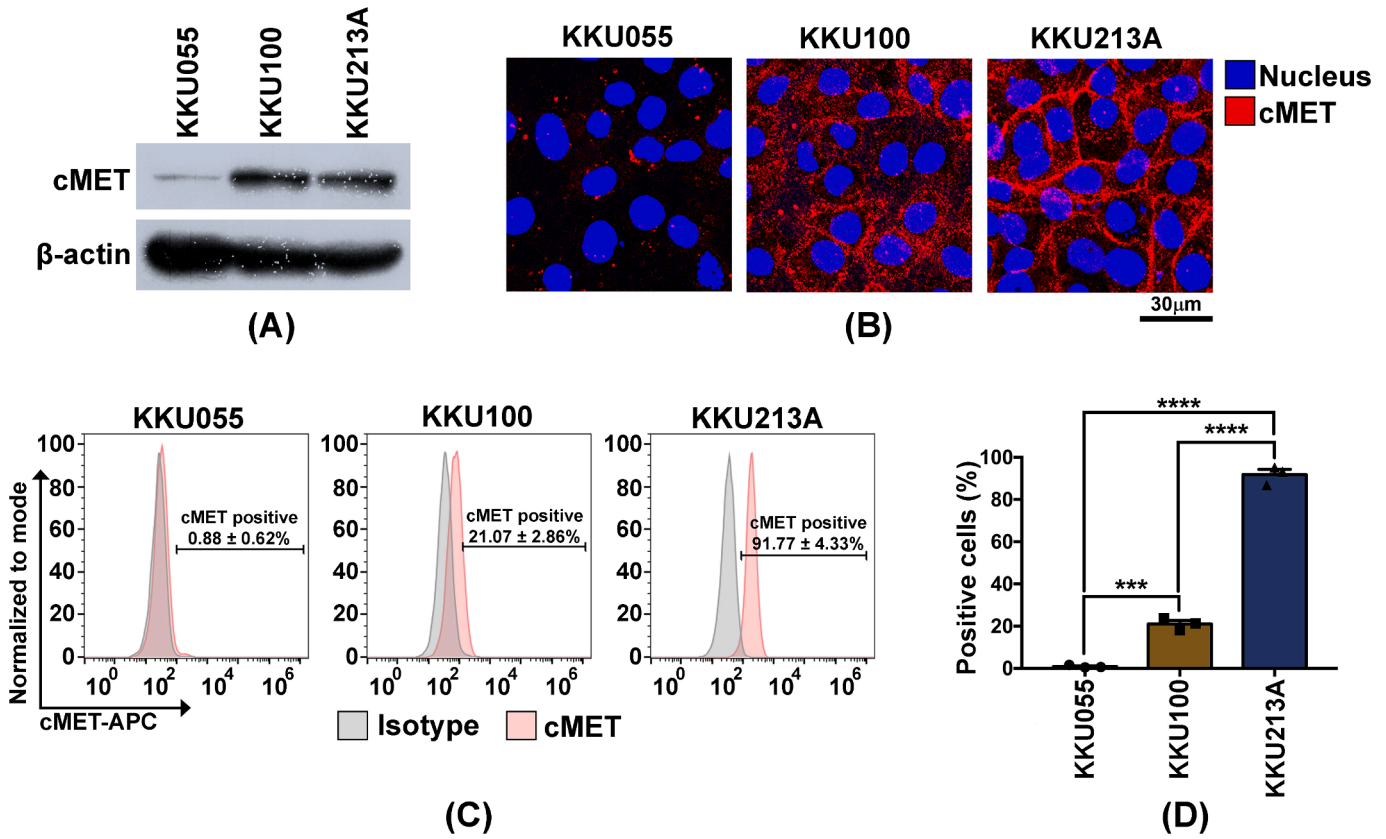

Fig. 1. Endogenous expression levels of cMET in CCA cell lines. The expression levels of cMET protein in KKU055, KKU100, and KKU213A were assessed through immunoblot assay (A), Immunofluorescence Assay (IFA) (B), and flow cytometry (C). The proportions of cMET-expressing cells are depicted (D). Statistical differences between groups are indicated, where *** denotes $p < 0.001$ and **** denotes $p < 0.0001$. In addition, the experiment was done in three independent experiment (N = 3).

measured by ELISA (Fig. 2D–E). The top three ScFv clones were identified: ScFv11 (2.053±0.20-fold), ScFv72 (1.85±0.37-fold), and ScFv114 (2.15±0.11-fold), showing strong binding activity compared to the control (Fig. 2E). Further examination of the binding efficiency of these ScFvs to the cMET protein on the surface of CCA cells was performed. Novel ScFv11, ScFv72, and ScFv114 were subsequently purified. The expression of purified ScFvs varied as observed by immunoblotting assay. Unfortunately, ScFv114 did not meet the minimum criteria for protein purification quality (Fig. 2F). Comparing the binding abilities of these ScFvs between KKU055 and KKU213A revealed that purified ScFv11 demonstrated a higher binding affinity to KKU213A (with the highest cMET expression) compared to KKU055 (with the lowest cMET expression), with binding levels of 19.83±0.27 % and 13.00±0.52 %, respectively. ScFv72 did not exhibit a statistically significant difference, with values of 10.30±0.84 % in KKU055 and 9.90 ±0.70 % in KKU213A (Fig. 2G).

3.3. Anti-cMET ScFvs bind to distinct epitopes on cMET proteins

Sequencing analysis was conducted to characterize the complementary determining regions (CDR) and framework regions (FR) of the selected ScFvs (ScFv11 and ScFv72) in comparison to a published sequence of a human ScFv targeted cMET (ScFvA) obtained from Liu *et al.* [28]. Nucleotide alignment results demonstrated differences in nucleotide arrangement. ScFv11 (735 bp encoding 245 amino acids) and ScFv72 (747 bp encoding 249 amino acids) exhibited slight similarity in the nucleotide sequence, while ScFvA (669 bp encoding 223 amino acids) displayed a shorter nucleotide sequence (Supplementary Fig. 2). Furthermore, amino acid sequence alignment was performed to compare the domain residues within the ScFv, including CDR and FR domains (Fig. 3). All ScFvs including ScFvA, ScFv11, and ScFv72, consisted of three CDR and four FR domains. ScFv11 and ScFv72 both strarted with the variable heavy chain (VH) domain, followed by the variable light chain (VL) domain, whereas ScFv A started with the variable light domain; V-kappa (VK) domain, and connected with VL.

Molecular docking analysis of novel ScFv11 and 72 was conducted to investigate their intermolecular interaction with cMET using the HADDOCK web-based software. The superimposition of the ScFvs (ScFvA, ScFv11, and ScFv72) displayed distinct interactions of individual ScFv against cMET (Fig. 4A–B). ScFvA utilized four residues (SER27, SER154, GLY155, and SRG202) to form three hydrogen bonds with four residues (SER531, ARG331, ARG469) of cMET, along with one Pi-charge (PHE97 – ASP469), and two hydrophobic interactions (LEU157 – ALA327 and VAL92 – PRO534) (Fig. 4C). The HADDOCK score for the ScFvA and cMET interaction was −69.8 ± 1.4. On the other hand, ScFv11 interacted with cMET using five residues (TYR96, GLY94, ASN161, ARG90, and GLY60) to form five hydrogen bonds with five residues of cMET (SER336, ARG331, LYS324, ASP449, and GLU549) (Fig. 4D). Additionally, an electrostatic interaction (ARG90 – ASP449) and hydrophobic interaction (ALA159 – ILE446, ILE337) were observed. The HADDOCK score for ScFv11 and cMET interaction was −65.9 ± 0.6. The docking result of ScFv72 and cMET revealed three hydrogen bonds between four residues of ScFv72 (TYR135, ASP131, TYR169, and TYR200) and three residues of cMET (GLN332, ARG331, and LEU337) (Fig. 4E). Moreover, a hydrophobic interaction was observed between ScFv72 (TRP70) and cMET (PHE373). The HADDOCK score for this interaction was −58 ± 1.0.

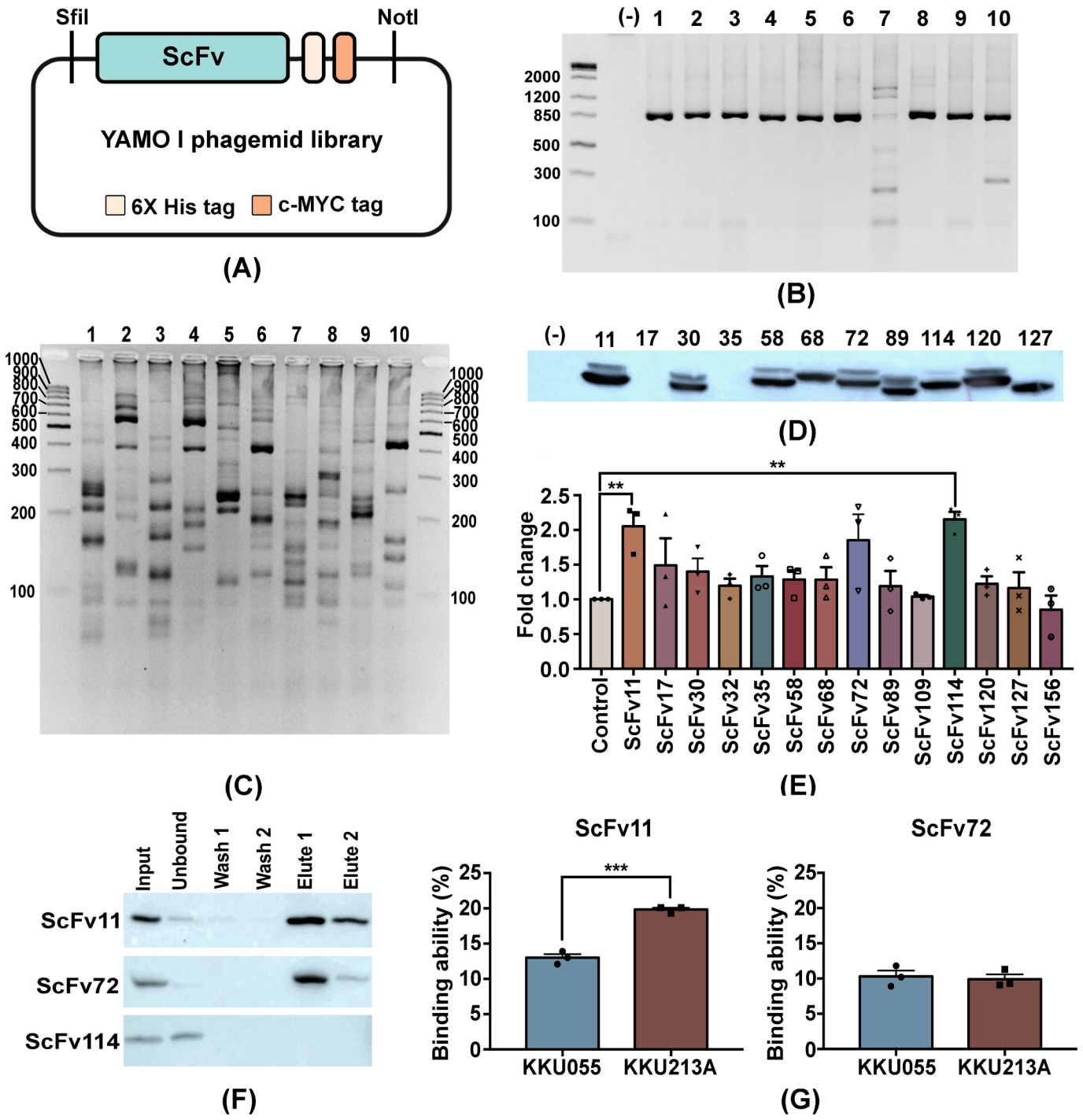

Fig. 2. Identification of novel humanized ScFvs targeting cMET. A. YAMO1 phage libraries consisting of pMOD1 phagemid vectors containing the ScFv domain with 6x His tag and MYC tag. B. Phage clones were screened by PCR to amplify the ScFv domain using specific universal primers, and PCR products were visualized by agarose electrophoresis. C. Restriction fragment length polymorphism (RFLP) patterns were observed after restriction enzyme digestion, visualized on a 3 % agarose gel. D. Secreted ScFvs in the culture supernatant of infected *E.coli* cells were detected and screened by immunoblot assay. E. The binding ability of ScFvs to cMET recombinant protein using ELISA technique. F. The top 3 ScFvs with the highest binding ability were purified. G. Purified proteins were confirmed for their binding ability to cMET-expressing CCA cell lines, comparing low cMET expressing KKU055 and high cMET expressing KKU213A. Statistical analysis compared the binding ability among samples which demonstrated in three independent experiments (** indicates $p < 0.01$ and *** indicates $p < 0.001$).

3.4. Anti-cMET CAR-NK-92 cells specifically eliminate cMET-Expressing CCA cells

The ScFvs targeting cMET (ScFvA, ScFv11, and ScFv72) were engineered to include a c-MYC tag and were then fused with a CAR cassette (Fig. 5A). The CAR cassette utilized in this study belonged to the second generation and consisted of a CD28 transmembrane domain, a 41BB costimulatory domain, and a CD3ζ signaling domain. Furthermore, the ScFv was connected to the CAR cassette through an IgG4 linker. Subsequently, the CAR constructs targeting cMET (referred to as anti-cMET CAR2) were integrated into the pcDH vector (Fig. 5B). The expression of anti-cMET CAR constructs was achieved through a transfection procedure in the Lenti-X^{TM} 293 T cell line, and the expression levels were assessed using IFA, immunoblot assay, and flow cytometry. The c-MYC-

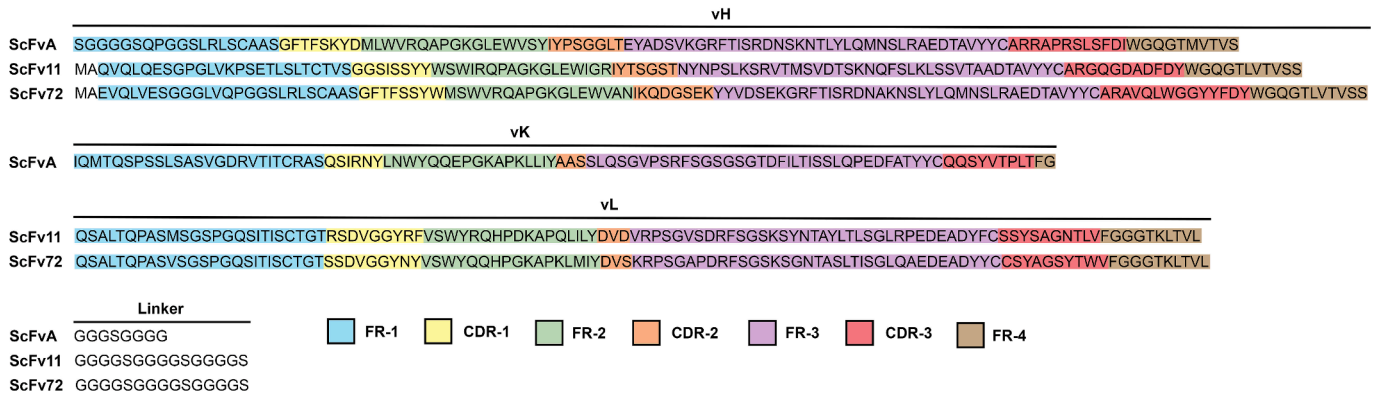

Fig. 3. Amino acid sequence alignment of ScFv domain. The VH, VL, and linker sequences of ScFv11 and ScFv72 were compared with ScFvA. The CDR and FR domain of each ScFv were predicted using the IgBlast databased [25].

tagged ScFv was used to visualize the expression of CAR constructs, represented in green (FITC) fluorescent color (Fig. 5C). Moreover, the expression of the entire CAR construct was confirmed by the detection of CD3ζ (Fig. 5D) at approximately 72 kDa. Finally, the transfection efficiency of the anti-cMET CAR2 constructs was investigated using flow cytometry. The anti-cMET CAR2 construct containing the ScFvA domain (A-CAR2) exhibited a positive expression rate of 80.23 ± 2.20 %, while the anti-cMET CAR2 constructs containing ScFv11 and ScFv72 displayed positive expression rates of 88.63 ± 2.77 % and 88.10 ± 0.72 %, respectively (Fig. 5E–F).

Considering that the highest expression of cMET was observed in KKU213A but not in KKU055, the specificity of the CAR-NK-92 cells was compared between KKU055 and KKU213A cell lines. A transduction procedure was conducted to generate anti-cMET CAR-NK-92 cells and evaluate the function of the novel ScFv against cMET (Fig. 6A and Supplementary Fig. 3). The histogram and bar graph in Fig. 6B and C illustrate the transduction efficiency of A-CAR2, 11-CAR2, and 72-CAR2, which were 38.00±4.95 %, 94.33±2.32 %, and 94.27±0.95 %, respectively. Initially, untransduced (UTD) NK-92 cells were cocultured with KKU055, KKU100, and KKU213A at various E:T ratios for 24 h. The cytotoxicity results indicated that at the E:T ratio of 2.5:1 resulted in percentages of target cell death that exceeded 75 % (Supplementary Figure 4). Therefore, E:T ratios of 0.5:1, 1:1, and 2:1 (all below 2.5:1) were selected to perform killing assays of anti-cMET CAR-NK-92 cells against KKU055 and KKU213A. The percentage of target cell death was determined by measuring the absorbance of crystal violet and calculating it using the aforementioned equation. The specificity of the novel ScFvs was further demonstrated by co-culturing anti-cMET CAR-NK-92 cells with KKU055 (the cell line with the lowest expression of cMET) (Fig. 6D) and KKU213A (which exhibits the highest level of cMET) (Fig. 6E). No statistically significant difference in target cell death was observed in the KKU055 cell line after cocultured with anti-cMET CAR-NK-92 cells compared with untransduced (UTD) control (67.76 ± 5.89 %) at an E:T ratio of 2:1. Interestingly, after co-culturing anti-cMET CAR-NK-92 cells with KKU213A at the highest E:T ratio, A-CAR2 and 11-CAR2 were able to significantly eliminate target cells, exhibiting target cell death rates of 84.74 ± 3.70 % and 79.88 ± 3.80 %, respectively, compared with UTD (64.71 ± 1.93 %).

4. Discussion

CAR-NK technology provides improved specificity and cytotoxicity against hematological malignancies and solid tumors [17]. In this investigation, the NK-92 cell line was selected as a model for CAR-NK therapy due to its homogenous population and demonstrated safety for allogeneic transfusion, even at high doses [33]. This published evidence highlights the potential of NK-92 cells as a readily available option for adoptive immunotherapy [17,33]. Expanding on these promising clinical outcomes, we further engineered NK-92 cells to augment their specificity and persistence by introducing CAR molecules [34]. Our CAR protein targeted cMET, a tyrosine kinase receptor whose aberrations have been implicated in various types of cancers. Upon binding of hepatocyte growth factor (HGF) to cMET, downstream signaling pathways, including STAT3 and PI3K/AKT, are activated through growth factor receptor-bound protein 2 (GRB2)-associated binding protein 1 (GAB1). These pathways mediate critical functions such as proliferation, differentiation, invasion, DNA repair, and survival of cancer cells [35]. cMET has come to attention for its high expression in CCA cells. In accompanied with clinical data, all CCA cell lines used in this study, including those originally established from Thai CCA and Japanese patients positively expressed cMET proteins (Supplementary Figure 5 and Supplementary Table 2). This result supports the concept of adopting cMET as a target for CCA. However, there was consistent variability observed in the expression levels of cMET across various CCA cell lines, underscoring their inherent heterogeneity [36]. Specifically, KKU213A, with a higher cMET expression than KKU055 and KKU100 demonstrates higher migratory and invasive capabilities [36,37]. Interestingly, migration and invasion which are crucial mechanism that promote metastasis in cancers [38], have been linked to the aberrant expression of the receptor tyrosine kinase cMET in CCA cells [39].

Several targeted therapies specific to cMET have been developed for CCA [40] including HGF/c-Met monoclonal antibody, soluble c-met receptor, and tyrosine kinase inhibitors [40]. Notably, c-MET inhibitors including tivantinib [22], LY2801653 [41], and cabozantinib have been employed in CCA treatment, however, these therapeutic approaches have not yielded satisfactory outcomes [42]. A Phase I study demonstrated a partial response in the combination treatment of escalating doses of tivantinib plus gemcitabine in only 20 % of patients with solid tumors including CCA (1 in 8 patients) [43]. Cabozantinib provided a median progression-free survival (PFS) of only 1.8 months [44], suggests a dubious clinical benefit of inhibiting c-Met signaling in the context of CCA. However, exploiting cMET overexpression in CCA, remains a promising therapeutic target for immunotherapy, particularly CAR-NK cell therapy. The engineering of CAR-NK-92 cells targeting cMET has produced a therapy option demonstrating specificity and enhanced anti-tumor activity against cMET overexpressing cancer cells such as lung adenocarcinoma [27] and liver cancer [28].

We have identified novel ScFv that specifically targets cMET from phage libraries displaying fully human ScFv (YAMO-library) [29] (Fig. 2). Compared with conventional murine monoclonal antibodies (mAb), humanized ScFv has been shown to offer superior functionality with lower immunogenicity [45], supporting their safe application in anti-cMET therapies. Comparing the previously reported ScFvA to our novel ScFv11 and ScFv72, the latter has a difference in the arrangement of VH and VL domains and complementarity determining regions (CDRs) which might affect their binding function [46,47]. Molecular

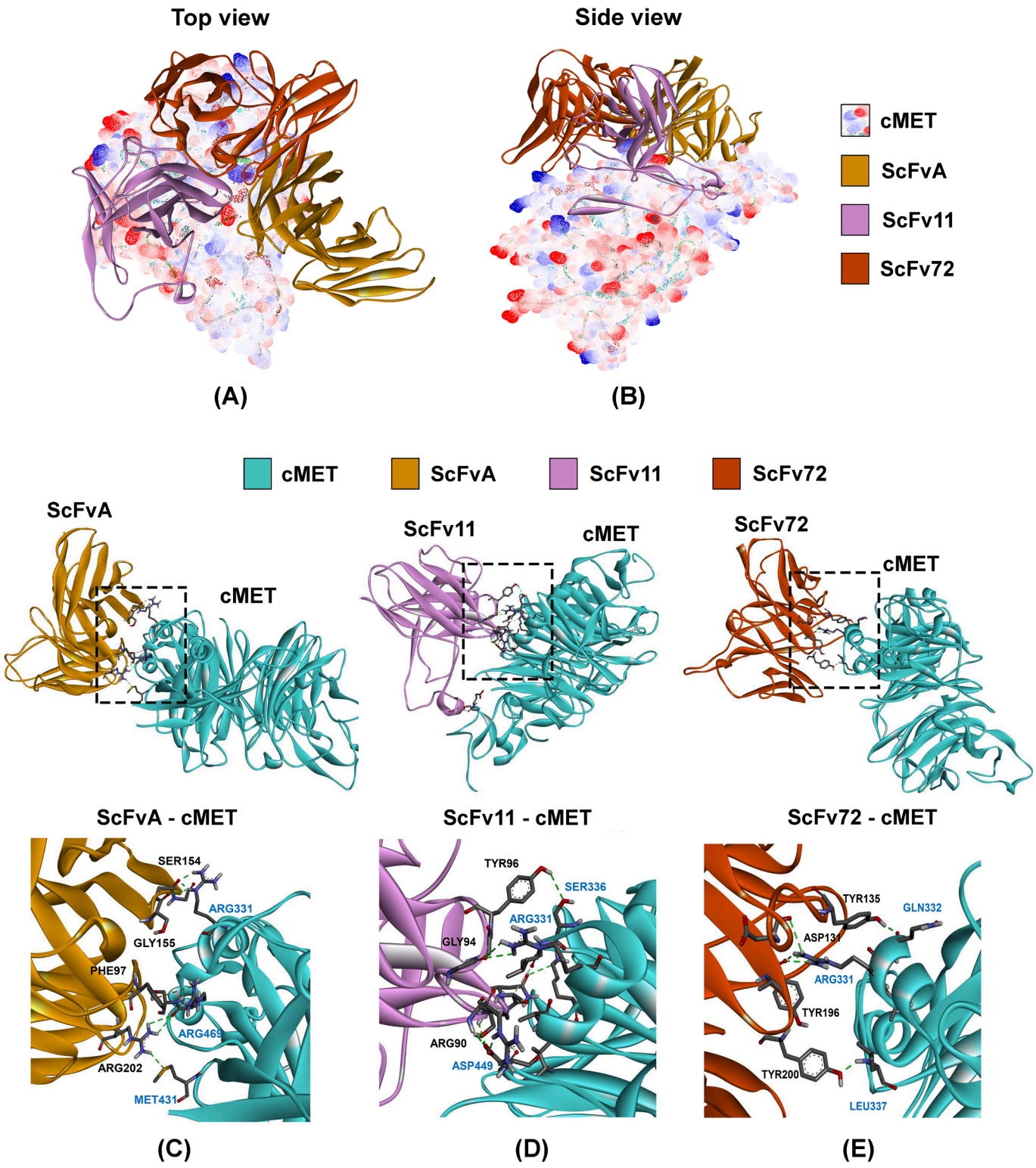

Fig. 4. Interaction of novel ScFv with human cMET protein. Molecular docking illustrates the interaction of ScFvA, ScFv11, or ScFv72 with cMET protein in the top view (A) and side view (B). The intermolecular interactions of ScFvA (C), ScFv11 (D), and ScFv72 (E) on cMET protein are depicted. The binding residues of ScFv and cMET are indicated in black and cyan colors. (For interpretation of the references to color in this figure legend, the reader is referred to the web version of this article.)

docking (Fig. 4) and cell-based ELISA results (Fig. 2 and Supplementary Figure 6) revealed ScFvA and ScFv11 achieved binding affinities higher than those of ScFv72. This strength of binding activity was crucial in boosting the anti-tumor activity of CAR-NK cells. Our result showed that anti-cMET CAR-NK-92 cells with A-CAR2 exhibited the most effective action in eliminating KKU213A followed by 11-CAR2 and 72-CAR2 (Fig. 6). This data emphasises the association between the activity of anti-cMET CAR-NK-92 cells and the binding affinity of the anti-cMET ScFv.

We generated anti-cMET CAR-NK-92 cells using a second-generation

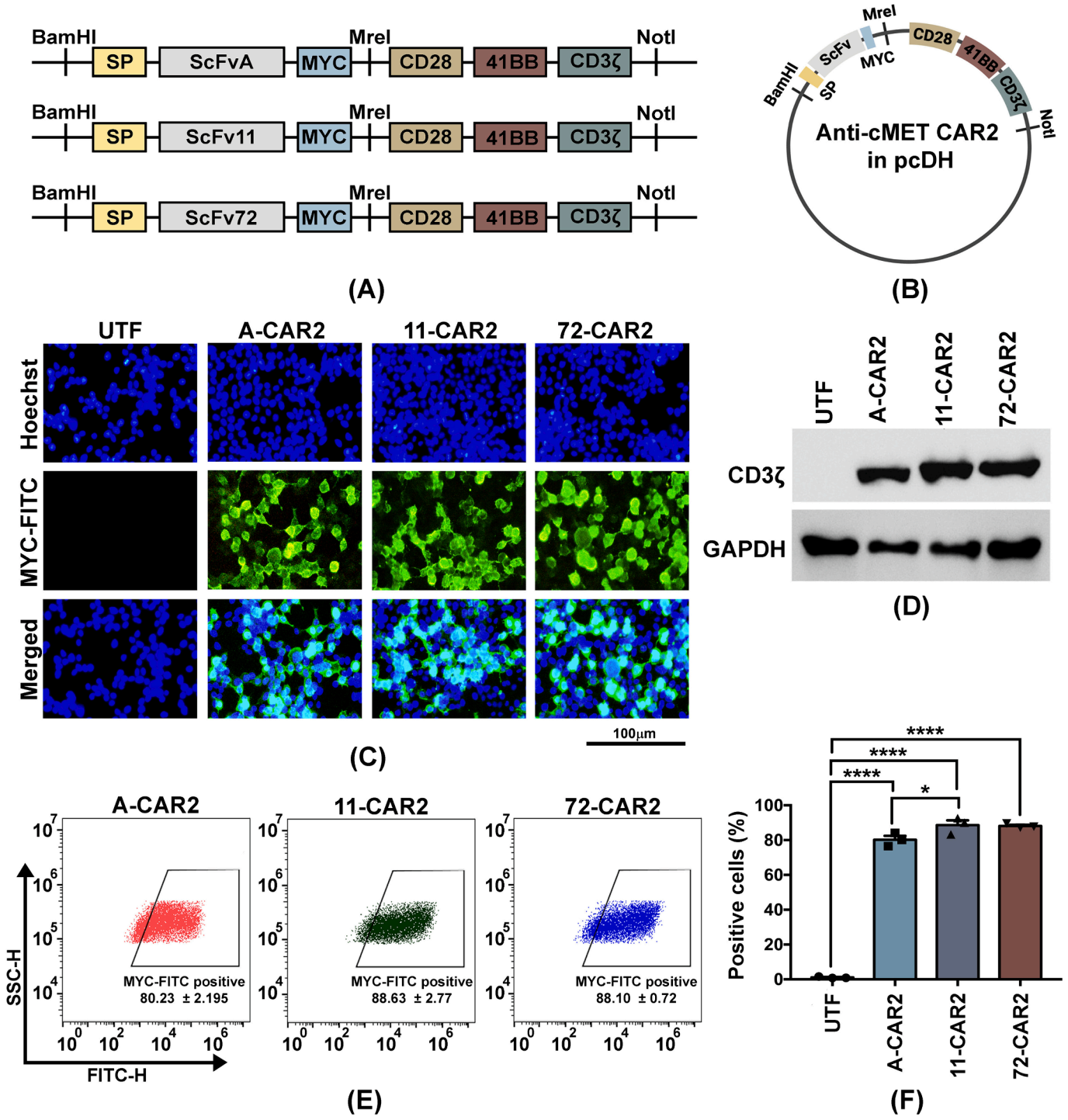

Fig. 5. Construction of anti-cMET CAR2 lentivirus vector. Selected ScFvs targeting cMET were incorporated into the CAR cassette (A) and subsequently linked to the pCDH lentivirus vector (B). The expression of anti-cMET CAR2 was assessed following transfection into lenti-X^{TM} 293 T cell lines using IFA (C), immunoblot (D), and flow cytometry (E). Transfection efficiencies were compared between untransfected controls (UTF) and cells transfected with CAR constructs (* indicates $p < 0.05$ and **** indicates $p < 0.0001$). The experiments were performed under three independent experiments (N = 3).

CAR construct containing the 41BB and CD3ζ domains. This generation of CAR is widely employed in both T [48] and NK cells [28] due to its robust anticancer efficacy against various cancer types [28,48–50]. While these domains originate from T cells, they have shown promising clinical outcomes in trials (NCT02839954, NCT02892695, NCT02742727, and NCT02944162) when introduced into NK cells [8]. Furthermore, the cytotoxic potential of CAR-NK cells can be enhanced by modifying the appropriate co-stimulatory domains [8]. Li and colleagues reported that CAR-NK containing the NKG2D transmembrane (TM) domain and 2B4 co-stimulatory domain improved anti-tumor activity against ovarian cancer by increased CD107a expression and IFN-gamma levels, ultimately resulting in prolonged *in vivo* survival in ovarian cancer model [51]. Our anti-cMET CAR-NK-92 cells with the second-generation CAR construct demonstrated high anti-tumor activity and their killing activity positively correlated with cMET expression level among target cells. Considering the low expression CCA, the

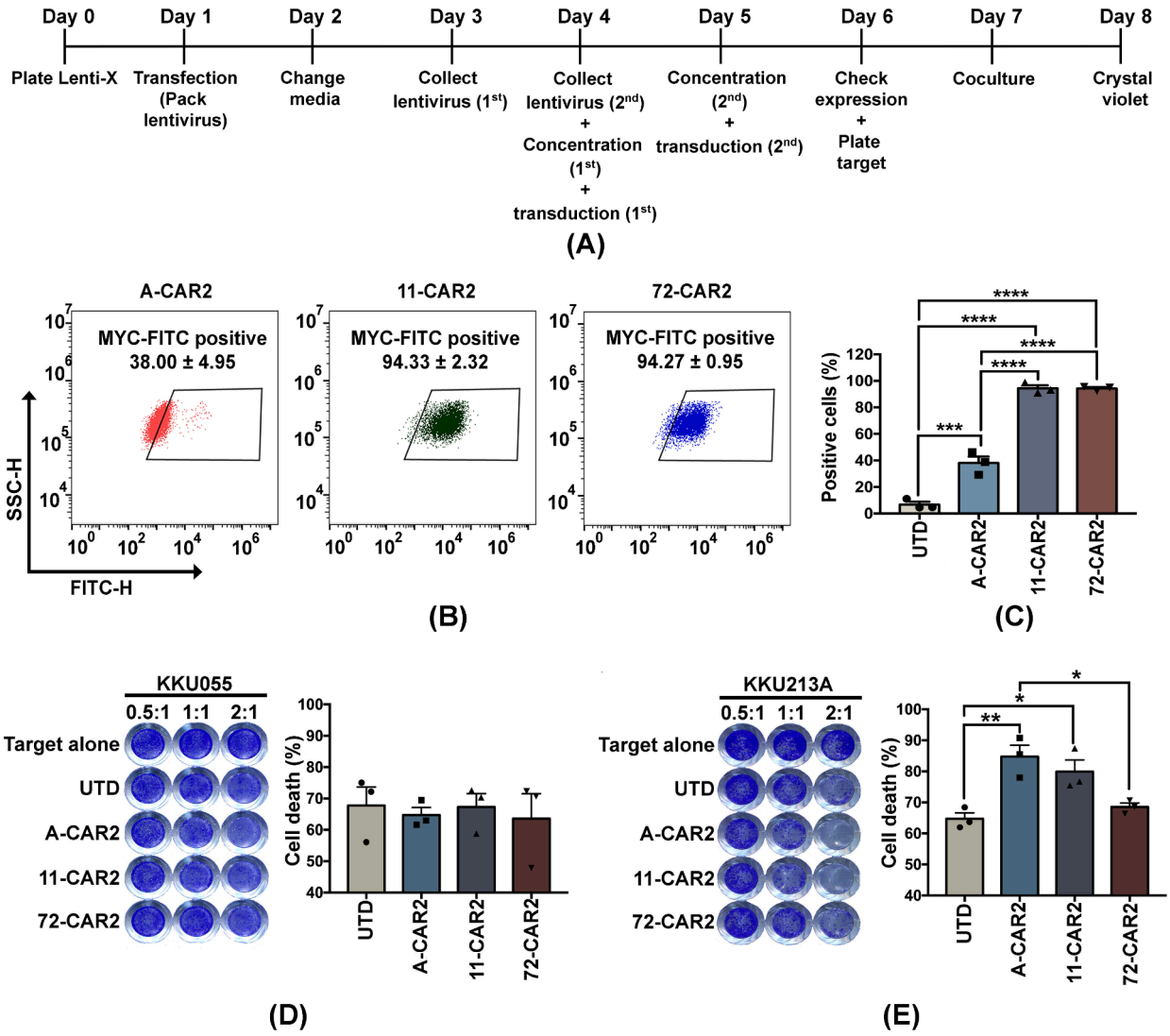

Fig. 6. Killing efficiency and specificity of anti-cMET CAR-NK-92 cells against CCA cell lines. A timeline illustrating the production of anti-cMET CAR-NK-92 cells, and the killing assay is presented (A). The transduction efficiency of anti-cMET CAR-NK-92 cells with A-CAR2, 11-CAR2, and 72-CAR2 was assessed by flow cytometry (B and C). The killing efficiency of CAR-NK-92 cells in eliminating CCA was compared between low cMET expressing KKU055 (D) and high cMET expressing KKU213A (E) cells after coculturing (* indicates $p < 0.05$, ** indicates $p < 0.01$, *** indicates $p < 0.001$, and **** indicates $p < 0.0001$). Three independent replications were performed in the experiment (N = 3).

combination approach with other immunotherapies to target different tumor antigens or combinations with standard chemotherapeutic drugs targeting survival/proliferation pathway should be considered. For instance, KKU055 exhibited a positive response to a combination treatment of genistein and NK-92 cells [52]. KKU100, which moderately expressed cMET, could alternatively be treated with a combination of gemcitabine and PD-L1xCD3 bispecific T cell engager (BiTE) [53].

It is crucial to acknowledge the potential of on-target, off-tumor toxicity during the use of anti-cMET CAR-NK92 cells, as cMET was found in adjacent normal tissue samples [23]. To minimize the risk of on-target, off-tumor toxicity, one potential strategy is to administer CAR-based immunotherapy via intratumoral injection. This approach could help minimize off-tumor side effect by targeting the therapy directly to the tumor site, thereby reducing exposure to normal tissues expressing the target antigen [54]. Another approach could be to adjust the binding affinity of ScFv to reduce the on-target, off-tumor toxicity [55]. Fine-tuning the affinity of ScFv for the target antigen may help enhance selectivity, allowing for preferential targeting of cancer cells while minimizing recognition of normal tissues expressing the antigen. For instance, HER2-CAR-T cells with lower binding affinity of HER2 ScFv were shown to increase sensitivity of HER2-CAR-T cells to HER2-high expressing tumors by discriminating between tumor cells expressing low- and high-level antigens [56]. The tumor xenograft NSG mice with human ovarian cancer cell lines, SK-OV3 (high HER2 expression) or human prostate cancer cells, PC3 (low HER2 expression), showed therapeutic efficacy of low affinity HER2-CAR-T cells to eliminate of HER2 overexpressed SK-OV3 but showed only limited reactivity against PC3 with physiological expression level of HER2 which emphasizing this strategy improve the safety profile and clinical outcome of CAR-NK cells. To assess the efficacy of our anti-cMET CAR-NK92 cells, including anti-tumor activity, circulation, tumor penetration, lifespan, and toxicity profiles, additional *in vivo* experiments in immunodeficient mouse models (such as NOG, NSG strains) would be beneficial. These models allow for the evaluation of the therapeutic potential and safety of the CAR-NK92 cells in a more physiological environment, providing valuable insights for further development and clinical translation.

In conclusion, this study identified novel anti-cMET ScFvs that exhibited specificity against cMET expressed on CCA cells. CAR-NK92 cells engineered with these anti-cMET ScFvs demonstrated efficiency in eliminating CCA cells, with effectiveness dependent on the expression

level of cMET on target cells. These findings suggest that anti-cMET CAR-NK92 cells could serve as an alternative treatment approach for CCA cases with high cMET expression, particularly in advanced stages where cMET expression correlates with disease progression. Moreover, considering the allogeneic properties and safety profile of NK-92 cells, our finding supports the potential of anti-cMET CAR-NK-92 therapy as an off-the-shelf immunotherapy option in the future. This therapy could be used either as adjuvant therapy alongside standard lines of treatment or in combination with other immunotherapy platforms, such as bi-specific T cells engager (BiTE) and/or tri-specific killer engager (TriKE), to maximize the therapeutic outcomes.

5. Authors' contributions

CC, MW, and NP designed and conducted the experiments, analyzed the data, interpreted the results, and draft the manuscript. MY provided phage libraries for anti-cMET ScFv screening. NS and AP performed phage display and bio-panning techniques. AP conceptualized and supervised the experiments. JS, MJ, JP, and PY provided materials/reagents and contributed to drafting the manuscript. AP and PY edited the manuscript. All authors have read and approved the final version of the manuscript submitted for journal publication.

Funding

This research work was supported by Chiang Mai University and partially supported by NSRF (Thailand National Science, Research, and Innovation Fund) via the Program Management Unit for Human Resources & Institutional Development, Research and Innovation [grant number B36G660005]. Pa-thai Yenchitsomanus is a member of the Thailand Hub of Talents in Cancer Immunotherapy (TTCI). The academic endeavors of TTCI receive support from the National Research Council of Thailand (N35E660102).

CRediT authorship contribution statement

Chutipa Chiawpanit: Writing – original draft, Methodology, Investigation. **Methi Wathikthinnakorn:** Writing – original draft, Methodology, Investigation. **Nunghathai Sawasdee:** Methodology, Investigation. **Nattaporn Phanthaphol:** Writing – original draft, Methodology, Investigation. **Jatuporn Sujjitjoon:** Resources. **Mutita Junking:** Resources. **Montarop Yamabhai:** Resources. **Jutatip Panaampon:** Resources. **Pa-thai Yenchitsomanus:** Writing – review & editing, Resources. **Aussara Panya:** Writing – review & editing, Writing – original draft, Supervision, Methodology, Investigation, Conceptualization.

Declaration of Competing Interest

The authors declare that they have no known competing financial interests or personal relationships that could have appeared to influence the work reported in this paper.

Data availability

Data will be made available on request.

Acknowledgments

We would like to express our sincere gratitude to Prof. George S. Baillie from the school of Cardiovascular and Metabolic Health, College of Medical, Veterinary and Life Sciences, University of Glasgow for his valuable assistance on language editing. We would like to thank the Office of Research Administration, Chiang Mai University, Chiang Mai, Thailand for supporting Chutipa Chiawpanit.

Appendix A. Supplementary material

Supplementary material to this article can be found online at https://doi.org/10.1016/j.intimp.2024.112273.

References

[1] B. Doherty, V.E. Nambudiri, W.C. Palmer, Update on the diagnosis and treatment of cholangiocarcinoma, Curr. Gastroenterol. Rep. 19 (1) (2017) 2.
[2] H. Malhi, G.J. Gores, Cholangiocarcinoma: modern advances in understanding a deadly old disease, J. Hepatol. 45 (6) (2006) 856–867.
[3] P.J. Brindley, M. Bachini, S.I. Ilyas, S.A. Khan, A. Loukas, A.E. Sirica, B.T. Teh, S. Wongkham, G.J. Gores, Cholangiocarcinoma, *Nat. Rev. Dis. Primers* 7 (1) (2021) 65.
[4] D. Moris, M. Palta, C. Kim, P.J. Allen, M.A. Morse, M.E. Lidsky, Advances in the treatment of intrahepatic cholangiocarcinoma: an overview of the current and future therapeutic landscape for clinicians, CA Cancer J. Clin. 73 (2) (2023) 198–222.
[5] X. Lei, Y. Lei, J.K. Li, W.X. Du, R.G. Li, J. Yang, J. Li, F. Li, H.B. Tan, Immune cells within the tumor microenvironment: biological functions and roles in cancer immunotherapy, Cancer Lett. 470 (2020) 126–133.
[6] E. Manthopoulou, D. Ramai, J. Dhar, J. Samanta, A. Ioannou, E. Lusina, R. Sacco, A. Facciorusso, Cholangiocarcinoma in the era of immunotherapy, Vaccines (Basel) 11 (6) (2023).
[7] S. Feins, W. Kong, E.F. Williams, M.C. Milone, J.A. Fraietta, An introduction to chimeric antigen receptor (CAR) T-cell immunotherapy for human cancer, Am. J. Hematol. 94 (S1) (2019) S3–S9.
[8] G. Xie, H. Dong, Y. Liang, J.D. Ham, R. Rizwan, J. Chen, CAR-NK cells: a promising cellular immunotherapy for cancer, EBioMedicine 59 (2020) 102975.
[9] S.L. Maude, T.W. Laetsch, J. Buechner, S. Rives, M. Boyer, H. Bittencourt, P. Bader, M.R. Verneris, H.E. Stefanski, G.D. Myers, et al., Tisagenlecleucel in children and young adults with B-cell lymphoblastic leukemia, N. Engl. J. Med. 378 (5) (2018) 439–448.
[10] S.J. Schuster, M.R. Bishop, C.S. Tam, E.K. Waller, P. Borchmann, J.P. McGuirk, U. Jäger, S. Jaglowski, C. Andreadis, J.R. Westin, et al., Tisagenlecleucel in adult relapsed or refractory diffuse large b-cell lymphoma, N. Engl. J. Med. 380 (1) (2019) 45–56.
[11] S.S. Neelapu, F.L. Locke, N.L. Bartlett, L.J. Lekakis, D.B. Miklos, C.A. Jacobson, I. Braunschweig, O.O. Oluwole, T. Siddiqi, Y. Lin, et al., Axicabtagene ciloleucel CAR T-cell therapy in refractory large b-cell lymphoma, N. Engl. J. Med. 377 (26) (2017) 2531–2544.
[12] J.S. Abramson, M.L. Palomba, L.I. Gordon, M.A. Lunning, M. Wang, J. Arnason, A. Mehta, E. Purev, D.G. Maloney, C. Andreadis, et al., Lisocabtagene maraleucel for patients with relapsed or refractory large B-cell lymphomas (TRANSCEND NHL 001): a multicentre seamless design study, Lancet 396 (10254) (2020) 839–852.
[13] M. Wang, J. Munoz, A. Goy, F.L. Locke, C.A. Jacobson, B.T. Hill, J.M. Timmerman, H. Holmes, S. Jaglowski, I.W. Flinn, et al., KTE-X19 CAR T-cell therapy in relapsed or refractory mantle-cell lymphoma, N. Engl. J. Med. 382 (14) (2020) 1331–1342.
[14] N.C. Munshi, L.D. Anderson Jr., N. Shah, D. Madduri, J. Berdeja, S. Lonial, N. Raje, Y. Lin, D. Siegel, A. Oriol, et al., Idecabtagene vicleucel in relapsed and refractory multiple myeloma, N. Engl. J. Med. 384 (8) (2021) 705–716.
[15] R.S. Siddiqui, M. Sardar, A systematic review of the role of chimeric antigen receptor T (CAR-T) cell therapy in the treatment of solid tumors, Cureus 13 (4) (2021) e14494.
[16] X. Peng, L. Chen, L. Chen, B. Wang, Y. Wang, X. Zhan, Chimeric antigen receptor-natural killer cells: novel insight into immunotherapy for solid tumors (review), Exp. Ther. Med. 21 (4) (2021) 340.
[17] K. Pan, H. Farrukh, V. Chittepu, H. Xu, C.X. Pan, Z. Zhu, CAR race to cancer immunotherapy: from CAR T, CAR NK to CAR macrophage therapy, J. Exp. Clin. Cancer Res. 41 (1) (2022) 119.
[18] S. Mori, H. Akita, S. Kobayashi, Y. Iwagami, D. Yamada, Y. Tomimaru, T. Noda, K. Gotoh, Y. Takeda, M. Tanemura, et al., Inhibition of c-MET reverses radiation-induced malignant potential in pancreatic cancer, Cancer Lett. 512 (2021) 51–59.
[19] D. Lau, H. Wadhwa, S. Sudhir, A.C. Chang, S. Jain, A. Chandra, A.T. Nguyen, J. M. Spatz, A. Pappu, S.S. Shah, et al., Role of c-Met/β1 integrin complex in the metastatic cascade in breast cancer, JCI Insight 6 (12) (2021).
[20] N. Boromand, M. Hasanzadeh, S. ShahidSales, M. Farazestanian, M. Gharib, H. Fiuji, N. Behboodi, N. Ghobadi, S.M. Hassanian, G.A. Ferns, et al., Clinical and prognostic value of the C-Met/HGF signaling pathway in cervical cancer, J. Cell Physiol. 233 (6) (2018) 4490–4496.
[21] A. Bahrami, S. Shahidsales, M. Khazaei, M. Ghayour-Mobarhan, M. Maftouh, S. M. Hassanian, A. Avan, C-Met as a potential target for the treatment of gastrointestinal cancer: current status and future perspectives, J. Cell Physiol. 232 (10) (2017) 2657–2673.
[22] K. Wei, M. Li, M. Zöller, M. Wang, A. Mehrabi, K. Hoffmann, Targeting c-MET by Tivantinib through synergistic activation of JNK/c-jun pathway in cholangiocarcinoma, Cell Death Dis. 10 (3) (2019) 231.
[23] Z.Y. Mao, G.Q. Zhu, L. Ren, X.C. Guo, D. Su, L. Bai, Prognostic value of c-met expression in cholangiocarcinoma, Technol. Cancer Res. Treat 15 (2) (2016) 227–233.
[24] N.-J. Chiang, C. Hsu, J.-S. Chen, H.-H. Tsou, Y.-Y. Shen, Y. Chao, M.-H. Chen, T.-S. Yeh, Y.-S. Shan, S.-F. Huang, et al., Expression levels of ROS1/ALK/c-MET and therapeutic efficacy of cetuximab plus chemotherapy in advanced biliary tract cancer, Sci. Rep. 6 (1) (2016) 25369.

[25] M. Miyamoto, H. Ojima, M. Iwasaki, H. Shimizu, A. Kokubu, N. Hiraoka, T. Kosuge, D. Yoshikawa, T. Kono, H. Furukawa, et al., Prognostic significance of overexpression of c-Met oncoprotein in cholangiocarcinoma, Br. J. Cancer 105 (1) (2011) 131–138.
[26] F. Moosavi, E. Giovannetti, L. Saso, O. Firuzi, HGF/MET pathway aberrations as diagnostic, prognostic, and predictive biomarkers in human cancers, Crit. Rev. Clin. Lab. Sci. 56 (8) (2019) 533–566.
[27] Y. Peng, W. Zhang, Y. Chen, L. Zhang, H. Shen, Z. Wang, S. Tian, X. Yang, D. Cui, Y. He, et al., Engineering c-Met-CAR NK-92 cells as a promising therapeutic candidate for lung adenocarcinoma, Pharmacol. Res. 188 (2023) 106656.
[28] B. Liu, Z.Z. Liu, M.L. Zhou, J.W. Lin, X.M. Chen, Z. Li, W.B. Gao, Z.D. Yu, T. Liu, Development of c-MET-specific chimeric antigen receptor-engineered natural killer cells with cytotoxic effects on human liver cancer HepG2 cells, Mol. Med. Rep. 20 (3) (2019) 2823–2831.
[29] P. Pansri, N. Jaruseranee, K. Rangnoi, P. Kristensen, M. Yamabhai, A compact phage display human scFv library for selection of antibodies to a wide variety of antigens, BMC Biotechnol. 9 (2009) 6.
[30] A. Waterhouse, M. Bertoni, S. Bienert, G. Studer, G. Tauriello, R. Gumienny, F. T. Heer, T.A.P. de Beer, C. Rempfer, L. Bordoli, et al., SWISS-MODEL: homology modelling of protein structures and complexes, Nucleic Acids Res. 46 (W1) (2018) W296–W303.
[31] B.G. Pierce, K. Wiehe, H. Hwang, B.H. Kim, T. Vreven, Z. Weng, ZDOCK server: interactive docking prediction of protein-protein complexes and symmetric multimers, Bioinformatics 30 (12) (2014) 1771–1773.
[32] C. Dominguez, R. Boelens, A.M.J.J. Bonvin, HADDOCK: a protein−protein docking approach based on biochemical or biophysical information, J. Am. Chem. Soc. 125 (7) (2003) 1731–1737.
[33] G. Suck, M. Odendahl, P. Nowakowska, C. Seidl, W.S. Wels, H.G. Klingemann, T. Tonn, NK-92: an 'off-the-shelf therapeutic' for adoptive natural killer cell-based cancer immunotherapy, Cancer Immunol. Immunother 65 (4) (2016) 485–492.
[34] A. Biederstädt, K. Rezvani, Engineering the next generation of CAR-NK immunotherapies, Int. J. Hematol. 114 (5) (2021) 554–571.
[35] P.M. Comoglio, L. Trusolino, C. Boccaccio, Known and novel roles of the MET oncogene in cancer: a coherent approach to targeted therapy, Nat. Rev. Cancer 18 (6) (2018) 341–358.
[36] B. Sripa, W. Seubwai, K. Vaeteewoottacharn, K. Sawanyawisuth, A. Silsirivanit, W. Kaewkong, K. Muisuk, P. Dana, C. Phoomak, W. Lert-Itthiporn, et al., Functional and genetic characterization of three cell lines derived from a single tumor of an opisthorchis viverrini-associated cholangiocarcinoma patient, Hum. Cell 33 (3) (2020) 695–708.
[37] N. Tepsiri, L. Chaturat, B. Sripa, W. Namwat, S. Wongkham, V. Bhudhisawasdi, W. Tassaneeyakul, Drug sensitivity and drug resistance profiles of human intrahepatic cholangiocarcinoma cell lines, World J. Gastroenterol. 11 (18) (2005) 2748–2753.
[38] K.T. Yeung, J. Yang, Epithelial-mesenchymal transition in tumor metastasis, Mol. Oncol. 11 (1) (2017) 28–39.
[39] K. Leelawat, S. Leelawat, P. Tepaksorn, P. Rattanasinganchan, A. Leungchaweng, R. Tohtong, P. Sobhon, Involvement of c-Met/hepatocyte growth factor pathway in cholangiocarcinoma cell invasion and its therapeutic inhibition with small interfering RNA specific for c-Met, J. Surg. Res. 136 (1) (2006) 78–84.
[40] M.P. Socoteanu, F. Mott, G. Alpini, A.E. Frankel, c-Met targeted therapy of cholangiocarcinoma, World J. Gastroenterol. 14 (19) (2008) 2990–2994.
[41] S. Barat, P. Bozko, X. Chen, T. Scholta, F. Hanert, J. Götze, N.P. Malek, L. Wilkens, R.R. Plentz, Targeting c-MET by LY2801653 for treatment of cholangiocarcinoma, Mol. Carcinog. 55 (12) (2016) 2037–2050.
[42] S. Rizvi, S.A. Khan, C.L. Hallemeier, R.K. Kelley, G.J. Gores, Cholangiocarcinoma—evolving concepts and therapeutic strategies, Nat. Rev. Clin. Oncol. 15 (2) (2018) 95–111.
[43] S. Pant, M. Saleh, J. Bendell, J.R. Infante, S. Jones, C.D. Kurkjian, K.M. Moore, J. Kazakin, G. Abbadessa, Y. Wang, et al., A phase I dose escalation study of oral c-MET inhibitor tivantinib (ARQ 197) in combination with gemcitabine in patients with solid tumors, Ann. Oncol. 25 (7) (2014) 1416–1421.
[44] L. Goyal, H. Zheng, M.B. Yurgelun, T.A. Abrams, J.N. Allen, J.M. Cleary, M. Knowles, E. Regan, A. Reardon, A. Khachatryan, et al., A phase 2 and biomarker study of cabozantinib in patients with advanced cholangiocarcinoma, Cancer 123 (11) (2017) 1979–1988.
[45] L. Huang, X. Su, H.J. Federoff, Single-chain fragment variable passive immunotherapies for neurodegenerative diseases, Int. J. Mol. Sci. 14 (9) (2013) 19109–19127.
[46] S.J. Kellmann, S. Dübel, H. Thie, A strategy to identify linker-based modules for the allosteric regulation of antibody-antigen binding affinities of different scFvs, MAbs 9 (3) (2017) 404–418.
[47] A. Gąciarz, L.W. Ruddock, Complementarity determining regions and frameworks contribute to the disulfide bond independent folding of intrinsically stable scFv, PLoS One 12 (12) (2017) e0189964.
[48] D.G. Song, Q. Ye, C. Carpenito, M. Poussin, L.P. Wang, C. Ji, M. Figini, C.H. June, G. Coukos, D.J. Powell Jr., In vivo persistence, tumor localization, and antitumor activity of CAR-engineered T cells is enhanced by costimulatory signaling through CD137 (4–1BB), Cancer Res. 71 (13) (2011) 4617–4627.
[49] S. Kong, S. Sengupta, B. Tyler, A.J. Bais, Q. Ma, S. Doucette, J. Zhou, A. Sahin, B. S. Carter, H. Brem, et al., Suppression of human glioma xenografts with second-generation IL13R-specific chimeric antigen receptor-modified T cells, Clin. Cancer Res. 18 (21) (2012) 5949–5960.
[50] H. Zhao, Z. Zhou, G. Li, G. Liu, S. Lin, W. Chen, S. Xiong, An NK cell line (NK92-41BB) expressing high levels of granzyme is engineered to express the high affinity chimeric genes CD16/CAR, Cytotechnology 73 (4) (2021) 539–553.
[51] Y. Li, D.L. Hermanson, B.S. Moriarity, D.S. Kaufman, Human iPSC-derived natural killer cells engineered with chimeric antigen receptors enhance anti-tumor activity, Cell Stem. Cell 23 (2) (2018) 181–192, e185.
[52] C. Chiawpanit, S. Panwong, N. Sawasdee, P.T. Yenchitsomanus, Panya A: genistein sensitizes human cholangiocarcinoma cell lines to be susceptible to natural killer cells, Biology (Basel) 11 (8) (2022).
[53] M. Wathikthinnakon, P. Luangwattananun, N. Sawasdee, C. Chiawpanit, V.S. Lee, P. Nimmanpipug, Y. Tragoolpua, S. Rotarayanont, T. Sangsuwannukul, N. Phanthaphol, et al., Combination gemcitabine and PD-L1xCD3 bispecific T cell engager (BiTE) enhances T lymphocyte cytotoxicity against cholangiocarcinoma cells, Sci. Rep. 12 (1) (2022) 6154.
[54] J. Tchou, Y. Zhao, B.L. Levine, P.J. Zhang, M.M. Davis, J.J. Melenhorst, I. Kulikovskaya, A.L. Brennan, X. Liu, S.F. Lacey, et al., Safety and efficacy of intratumoral injections of chimeric antigen receptor (CAR) T cells in metastatic breast cancer, Cancer Immunol. Res. 5 (12) (2017) 1152–1161.
[55] Y. Duan, R. Chen, Y. Huang, X. Meng, J. Chen, C. Liao, Y. Tang, C. Zhou, X. Gao, J. Sun, Tuning the ignition of CAR: optimizing the affinity of scFv to improve CAR-T therapy, Cell Mol. Life Sci. 79 (1) (2021) 14.
[56] X. Liu, S. Jiang, C. Fang, S. Yang, D. Olalere, E.C. Pequignot, A.P. Cogdill, N. Li, M. Ramones, B. Granda, et al., Affinity-Tuned ErbB2 or EGFR chimeric antigen receptor t cells exhibit an increased therapeutic index against tumors in mice, Cancer Res. 75 (17) (2015) 3596–3607.